A&A manuscript no.
(will be inserted by hand later)

Your thesaurus codes are:
08 (08.01.03; 08.06.03; 08.12.02; 08.09.02)

ASTRONOMY AND ASTROPHYSICS
January 10, 2000

On the Interpretation of the Optical Spectra of L-type Dwarfs*

Ya. Pavlenko[1], **M. R. Zapatero Osorio**[2], and **R. Rebolo**[2,3]

[1] Main Astronomical Observatory, Golosiiv, 03680 Kyiv-127, Ukraine
[2] Instituto de Astrofísica de Canarias. C/. Vía Láctea s/n, E-38200 La Laguna, Tenerife. Spain
[3] Consejo Superior de Investigaciones Científicas, Spain

Accepted for publication in A&A, 4 Jan 00

Abstract. We present synthetic optical spectra in the red and far-red (640–930 nm) of a sample of field L dwarfs suitably selected to cover this new spectral class, and the brown dwarf GL 229B. We have used the recent "dusty" atmospheres by Tsuji (2000) and by Allard (1999), and a synthesis code (Pavlenko et al. 1995) working under LTE conditions which considers the chemical equilibrium of more than 100 molecular species and the detailed opacities for the most relevant bands. Our computations show that the alkali elements Li, Na, K, Rb, and Cs govern the optical spectra of the objects in our sample, with Na and K contributing significantly to block the optical emergent radiation. Molecular absorption bands of oxides (TiO and VO) and hydrides (CrH, FeH and CaH) also dominate at these wavelengths in the early L-types showing a strength that progressively decreases for later types. We find that the densities of these molecules in the atmospheres of our objects are considerably smaller by larger factors than those predicted by chemical equilibrium considerations. This is consistent with Ti and V atoms being depleted into grains of dust.

In order to reproduce the overall shape of the optical spectra of our observations an additional opacity is required to be implemented in the computations. We have modelled it with a simple law of the form $a_\circ\ (\nu/\nu_\circ)^N$, with $N = 4$, and found that this provides a sufficiently good fit to the data. This additional opacity could be due to molecular/dust absorption or to dust scattering. We remark that the equivalent widths and intensities of the alkali lines are highly affected by this opacity. In particular, the lithium resonance line at 670.8 nm, which is widely used as a substellarity discriminator, is more affected by the additional opacity than by the natural depletion of neutral lithium atoms into molecular species. Our theoretical spectra display a rather strong resonance feature even at very cool effective temperatures ($\sim$1000 K); depending on the effective temperature and on the amount of dust in the atmospheres of very cool dwarfs, it might be possible to achieve the detection of lithium even at temperatures this cool. Changes in the physical conditions governing dust formation in L-type objects will cause variability of the alkali lines, particularly of the shorter wavelength lines.

Key words: Stars: atmospheres; fundamental parameters; low-mass, brown dwarfs; individual: BRI 0021–0214, Gl 229B, Kelu 1, DenisP J1228–1547, DenisP J0205–1159

1. Introduction

The optical spectra of the recently discovered very cool dwarfs present new challenges to theoretical interpretation. Their spectral characteristics are drastically different from those of the well known M-dwarfs and this has prompted the use of a new spectral classification, the so-called L-dwarfs (Martín et al. 1997a, 1999; Kirkpatrick et al. 1999a). In principle, the study of the optical spectral energy distribution may allow a better understanding of their physical properties, effective temperatures, gravities, atmospheric composition, etc. The main molecular absorbers at optical wavelengths in early- to mid-M dwarfs are significantly depleted at the lower temperatures present in L dwarfs because of the incorporation of their atoms into dust grains. This process should start in the latest M-dwarf atmospheres (Lunine et al. 1989; Tsuji, Ohnaka & Aoki 1996a; Tsuji et al. 1996b; Jones & Tsuji 1997; Allard et al. 1997), considerably reducing the strength of TiO, VO and other molecular bands, and producing significant changes in the overall properties of

Send offprint requests to: R. Rebolo, M. Zapatero Osorio, Ya. Pavlenko

* Based on observations made with the William Herschel Telescope (WHT) operated on the island of La Palma by the Isaac Newton Group at the Observatorio del Roque de los Muchachos of the Instituto de Astrofísica de Canarias; and on observations obtained at the W. M. Keck Observatory, which is operated as a scientific partnership among the California Institute of Technology, the University of California and the National Aeronautics and Space Administration. This observatory was made possible by the generous financial support of the W. M. Keck Foundation.

Correspondence to: rrl@iac.es,mosorio@iac.es,yp@mao.kiev.ua

Table 1. Log of spectroscopic observations

Object	Spec. Type	Telescope	Dispersion (Å/pix)	$\Delta\lambda$ (nm)	Date (1997)	Exposure (s)
Kelu 1	L2 (L2)	WHT	2.9	640–930	Jun 16	2×1200
Denis-P J1228–1547	L4.5 (L5)	WHT	2.9	640–930	Jun 14	2×1200
Denis-P J0205–1159	L5 (L7)	WHT	2.9	640–930	Aug 23	2×1800
		KeckII	2.5	640–890	Nov 2	1×1600

NOTES. Spectral types are given in Martín et al. (1999). Those spectral types in brackets come from Kirkpatrick et al. (1999a).

the optical spectra. Naturally, the appearance of dust will modify the temperature structure of the atmosphere, significantly affecting the formation of the emerging spectrum (Allard et al. 1997).

In this paper we follow a semi-empirical approach to understand the relevance of different processes on the resulting spectral energy distributions in the optical for L dwarfs and Gl 229B. We have obtained far-red optical spectra of several of these cool dwarfs and compared them to synthetic spectra generated using the latest models by Tsuji (2000) and Allard (1999). These models have been successfully used in the interpretation of the near-infrared spectra of these objects (Tsuji, Ohnaka & Aoki 1999; Kirkpatrick et al. 1999b).We have taken into account the depletion of some relevant molecules associated with the formation of dust and we have investigated the effects of dust scattering and/or absorption on the formation of the optical spectra. Remarkably strong alkali lines are present in the spectra and dominate its shape in the 600–900 nm region, providing major constraints to the theoretical modelling. We present the observations in section 2, models and synthetic spectra in section 3, and the role of alkalis, molecular bands and dust scattering and/or absorption is considered in section 4. In section 5 we discuss the implications of our study on the determination of effective temperatures and gravities as well as the formation of the lithium resonance line which is a key discriminator of substellar nature in these objects. Finally, conclusions are presented in Section 6.

2. Observations and data reduction

We have collected intermediate-resolution spectra in the 640–930 nm range for Kelu 1 (Ruiz, Leggett & Allard 1997), Denis-P J1228–1547 and Denis-P J0205–1159 (Delfosse et al. 1997) using the 4.2 m William Herschel Telescope (WHT; Observatorio del Roque de los Muchachos, La Palma). The coolest L dwarf in our sample, Denis-P J0205–1159, has also been observed with the KeckII telescope (Mauna Kea Observatory, Hawaii). Table 1 summarizes the log of the observations. The instrumentation used was the ISIS double-arm spectrograph at the WHT (only the red arm) with the grating R158R and a TEK (1024×1024 pix^2) CCD detector, and the Low Resolution Imaging Spectrograph (LRIS, Oke et al. 1995) with the 600 grove mm^{-1} grating and the TEK (1024×1024 pix^2) CCD detector at the KeckII telescope. The nominal dispersion and the wavelength coverage provided by each instrumental setup were similar and are listed in Table 1. Slit projections were typically 2–3 pix giving spectral resolutions of 6–8 Å. Spectra were reduced by a standard procedure using IRAF[1], which included debiasing, flatfielding, optimal extraction, and wavelength calibration using the sky lines appearing in each individual spectrum (Osterbrock et al. 1996). Finally, the observed WHT spectra were corrected from instrumental response making use of the spectrophotometric standard stars BD +26° 2606 and HD 19445 which have absolute flux data available in the IRAF environment. No flux standards were observed at the KeckII telescope, and thus the instrumental signature of the KeckII spectrum of Denis-P J0205–1159 was removed by matching it with the WHT spectrum. Our observations are displayed in Fig. 1 together with spectra of the other two objects in our sample: BRI 0021–0214 (M9.5, Irwin, McMahon, & Reid 1991), and Gl 229B (a brown dwarf with methane absorptions, Nakajima et al. 1995; Oppenheimer et al. 1995). Our sample covers a wide range of spectral types, from the transition objects between M and L types down to the latest types.

3. Model atmospheres, spectral synthesis code, chemical equilibrium and opacities

We carried out the computations using the LTE spectral synthesis program WITA5, which is a modified version of the program used by Pavlenko et al. (1995) for the study of the formation of lithium lines in cool dwarfs. The modifications were aimed to incorporate "dusty effects" which can affect the chemical equilibrium and radiative transfer processes in very cool atmospheres. We have used the set of Tsuji's (2000) "dusty" (C-type) LTE model atmospheres. These models were computed for the case of segregation of dust–gas phases, i.e. for conditions $r_{dust} > r_{crit}$, where r_{dust} is the size of dust particles and r_{crit} is critical

[1] IRAF is distributed by National Optical Astronomy Observatories, whcih is operated by the Association of Universities for Research in Astronomy, Inc., under contract with the National Science Foundation.

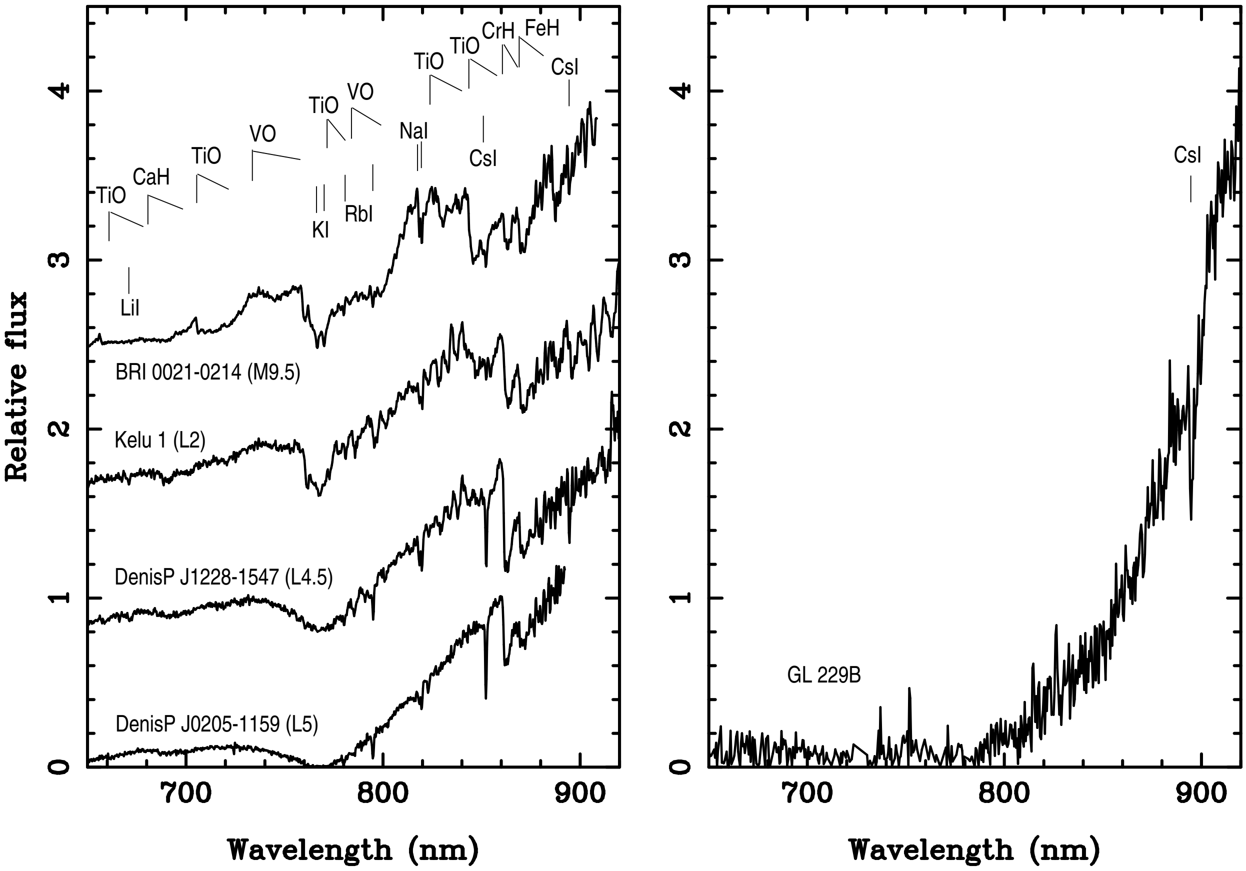

Fig. 1. Far-red optical spectra for our sample. New observations are those of Kelu 1, Denis-P J1228–1547 and Denis-P J0205–1159 (KeckII spectrum). Data for BRI 0021-0214 and Gl 229B have been collected from Martín, Rebolo & Zapatero Osorio (1996) and from Schultz et al. (1998), respectively. Spectral types for the L-dwarfs are given following the classification of Martín et al. (1999). Spectra in the left panel have been shifted by 0.8 units for clarity. Identification of some atomic and molecular features is provided in the top.

size corresponding to the gas–dust detailed equilibrium state. In a previous study (Pavlenko, Zapatero Osorio & Rebolo 2000) we had used Tsuji's (2000) B-type models which are computed for the case of $r_{dust} = r_{crit}$. In this paper we have also used a grid of the NextGen "dusty" model atmospheres computed recently by Allard (1999). The temperature-pressure stratification of Allard's models lie between those of the C-type and B-type models of Tsuji (2000) as it can be seen in Fig. 2.

Chemical equilibrium was computed for the mix of ≈100 molecular species. Alkali-contained species formation processes were considered in detail because of the important role of the neutral alkali atoms in the formation of the spectra. Constants for chemical equilibrium computations were taken mainly from Tsuji (1973).

In the high pressure conditions of the atmospheres of L-dwarfs some molecules can be oversaturated (Tsuji et al. 1996a); in this case such molecules should undergo condensation. To take into account this effect, we reduced the abundances of those molecular species down to the equilibrium values (Pavlenko 1998). The constants for computations of saturation densities were taken from Gurwitz et al. (1982).

We used the set of continuum opacity sources listed in Table 2 where we also give the original sources for the opacity computation codes. That opacity grid allows us to obtain resonable fits to a variety of stars (see e.g. Martín et al. 1997b; Israelian, García López & Rebolo 1998; Yakovina & Pavlenko 1998). Opacities due to molecular band absorption were treated using the Just Overlapping Line Approximation (JOLA). Synthetic spectra of late M-dwarfs using both the continuum opacities listed in Table 2 and the JOLA treatment for molecular band absorptions have been already discussed in Pavlenko (1997).

The alkali line data were taken from the VALD database (Piskunov et al. 1995, see their Table 3). At the low temperatures of our objects we deal with saturated absorption lines of alkalis. Their profiles are pressure broadened. At every depth in the model atmosphere the profile of the aborption lines is described by a Voigt function $H(a, v)$, where damping constants a were computed as in Pavlenko et al. (1995).

Table 2. List of the opacity sources used in our computations

Opacity source	Subprogram	Author
Bound-free absorption of H	HOP	Kurucz (1993)
H_2^+ absorption	H2PLOP	Kurucz (1993)
H^- ion absorption	HMINOP	Kurucz (1993)
Rayleigh scattering by H atoms	HRAYOP	Kurucz (1993)
He I bound-free absorption	HE1OP	Kurucz (1993)
He II bound-free absorption	HE2OP	Kurucz (1993)
He^- absorption	HEMIOP	Kurucz (1993)
Rayleigh scattering by He	HERAOP	Kurucz (1993)
Bound-free absorption ofMg I, Al I, Si I, Fe I, OH and CH	COOLOP	Kurucz (1993)
Bound-free absorption of N I, O I, Mg II, Si II, Ca I	LUKEOP	Kurucz (1993)
Bound-free absorption of C II + N II + O II	HOTOP	Kurucz (1993)
Electron Thompson scattering by e^-	ELECOP	Kurucz (1993)
Rayleigh scattering by H_2	H2RAOP	Kurucz (1993)
Absorption due to Hydrogen lines,	HLINOP	Kurucz (1993)
H_2 quasimolecule absorption	QUASIH	Pavlenko (1999a)
C^- ion absorption	CMINUSOP	Pavlenko (1999a)
Bound-free of C I	C1OPAC	Pavlenko (1999a)

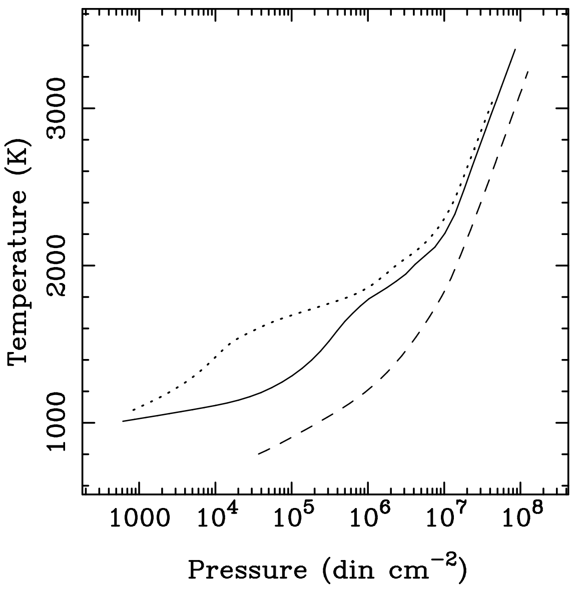

Fig. 2. Temperature structures for the model atmospheres of $T_{\rm eff} = 1400$ K and $\log g = 5.0$ given by Tsuji (2000, C-type, dashed line; B-type, dotted line) and by Allard (1999, full line).

3.1. Molecular opacities

Detail molecular opacities have been computed for all the molecules listed in Table 2 of Pavlenko et al. (1995) as well as for CrH and CaH. To compute the opacity due to absorption of VO and TiO bands we followed the scheme presented in Pavlenko et al. (1995) and Pavlenko (1997). However, for the $B^4\Pi_{(r)} - X^4\Sigma^-$ band system of VO we used a more complete matrix of Franc-Condon Factors computed by the FRANK program (Cymbal 1977) with account of rotational-vibrational interaction in the Morse-Pekeris approximation modified by Schumaker (1969, see Pavlenko 1999b for more details). Futhermore for this band system we used oscillator strength f_e from Allard & Hauschildt (1995). For the ϵ band system of TiO the parameters of Schwenke (1998) were used.

Table 3. List of atomic lines used in our computations

	λ_{vac} (nm)	gf	E'' (eV)
Li I	610.5164	0.126 E+01	1.840
Li I	610.5275	0.229 E+01	1.850
Li I	610.5290	0.257 E+00	1.850
Li I	670.9551	9.790 E−01	0.000
Li I	670.9701	4.900 E−01	0.000
Li I	812.8408	0.216 E+00	1.850
Li I	812.8629	0.432 E+00	1.850
Na I	589.1518	1.288 E+00	0.000
Na I	589.7489	6.457 E−01	0.000
Na I	819.6986	3.390 E−01	2.105
Na I	819.7016	3.090 E+00	2.105
Na I	818.5443	1.690 E+00	2.100
K I	766.6961	1.340 E+00	0.000
K I	770.1031	6.760 E−01	0.000
Rb I	780.2348	1.370 E+00	0.000
Rb I	794.9729	6.800 E−01	0.000
Cs I	894.5900	7.800 E−01	0.000
Cs I	852.3285	1.620 E+00	0.000

The CrH molecular band opacity was also considered, the data required for the computations of the electronic transition $A^6\Sigma^{(+)}$–$X^6\Sigma^{(+)}$ being taken from Huber & Herzberg (1979). Franc-Condon factors were computed by the FRANK program (Cymbal 1977). For this band system we used $f_e = 0.001$, determined by Pavlenko (1999b). Molecular bands of the $A^6\Sigma^{(+)}$–$X^6\Sigma^{(+)}$ of CrH lie in the wide wavelength region 500–1200 nm, and a head of the strong (0,1) band lies near the core of the K I atomic line. A head of the (0,0) band of $A^6\Sigma^{(+)}$–$X^6\Sigma^{(+)}$ system of CrH at 860 nm is blended with the heads of (1,0), (3,2), (2,1) bands of the $B^4\Pi_{(r)}$–$X^4\Sigma^-$ system of VO. For the spectral region 650–710 nm we took into account the absorption due to the $B^2\Sigma$–$X^2\Sigma$ band system of CaH for which we adopted $f_e = 0.05$. Frank-Condon factors were computed with the FRANK program. Although FeH is an important absorber at wavelengths around 870 nm and 990 nm for the coolest dwarfs, it is not yet included in our calculations due to the lack of appropriate laboratory data. In the wavelength region presented in this paper, the blue band of FeH is blended with CrH and VO.

4. Analysis and interpretation

4.1. Atomic features

Our spectral synthesis for model atmospheres in the temperature range 2200–1000 K confirms the relevant role of atomic features due to the Na I and K I resonance doublets in the spectral range 640–930 nm. The strength of these doublets increases dramatically when decreasing the effective temperature ($T_{\rm eff}$). In Fig. 3 we display synthetic spectra for different $T_{\rm eff}$ and gravity values. These computations do not include any molecular or grain opacity in order to show how alkali absorptions change with these parameters. In addition, we can see in the figure how the overall shape of the coolest L-dwarf spectra is governed by the resonance absorptions of Na I and K I. Even the less abundant alkali (i.e. Li, Rb, Cs) produce lines of remarkable strength. Note the increase in intensity of K I and Na I lines with decreasing $T_{\rm eff}$ and with increasing atmospheric gravity. Although this different behaviour can, in principle, make it difficult to disentangle these parameters from the optical spectra, simple physical considerations give an upper limit to gravity of $\log g = 5.5$ for brown dwarfs with lithium and therefore the large broadening of the K I lines seen in some of our objects cannot be attributed to higher aphysical values of gravity.

Our computations provide a qualitative explanation of the far-red spectral energy distributions presented in Fig. 1. The equivalent widths (EWs) of the K I and Na I resonance doublets may reach several thousand Angstroms, becoming the strongest lines so far seen in the spectra of astronomical objects. This is mainly caused by the high pressure broadening in the atmospheres of the coolest dwarfs, where damping constants of the absorption lines vary from 0.001 in the uppermost layer of the atmosphere to 2–4 in the deepest regions. The subordinate lines of Na I at 819.5 nm, clearly seen in all the L-dwarfs in our sample, become weaker as $T_{\rm eff}$ decreases. These computations also show that the subordinate Li I line at 812.6 nm may be detected in early/mid L-dwarfs with equivalent widths not exceeding 1Å, and that the triplet at 610.3 nm appears completely embedded by the wings of the K I and Na I resonance lines.

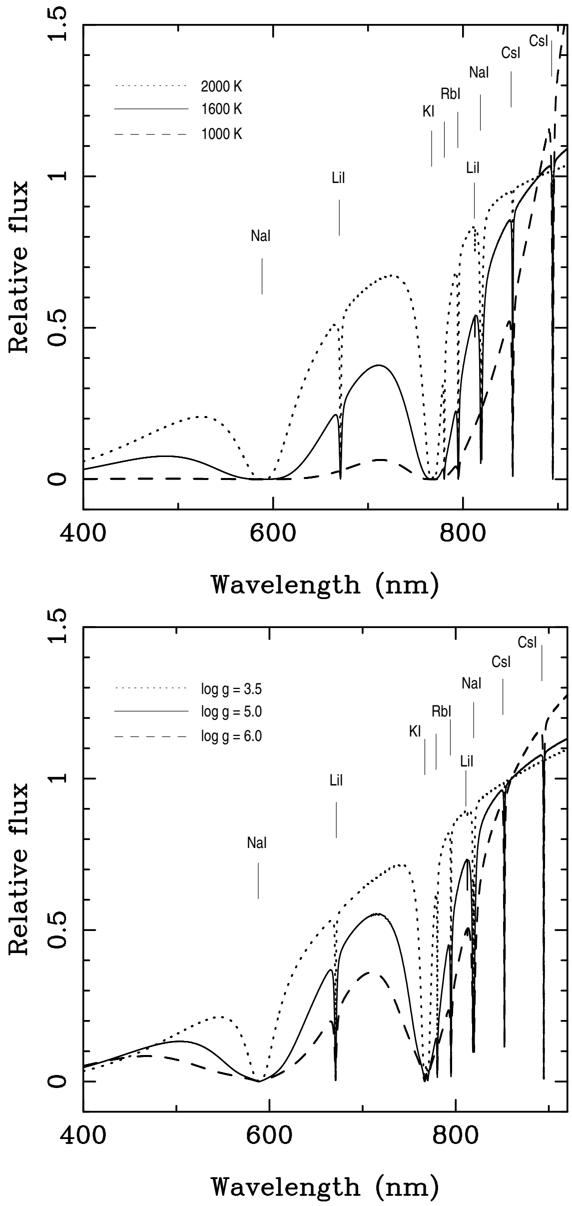

Fig. 3. Theoretical optical spectra for the alkali elements computed with different values of $T_{\rm eff}$ and gravity. The upper panel shows the dependence with temperature (computations performed using Tsuji's 2000 C-type models and $\log g = 5.0$. Spectra are normalized at 880 nm). The lower panel displays the dependence with gravity at $T_{\rm eff} = 1600$ K (Allard's 1999 "dusty" models. Spectra are normalized at 860 nm). Identifications of the atomic lines are given in the top.

4.2. Molecular features

In the optical spectra of very cool dwarfs one expects the presence of bands of VO, TiO and indeed, our synthetical spectra show that these bands play an important role

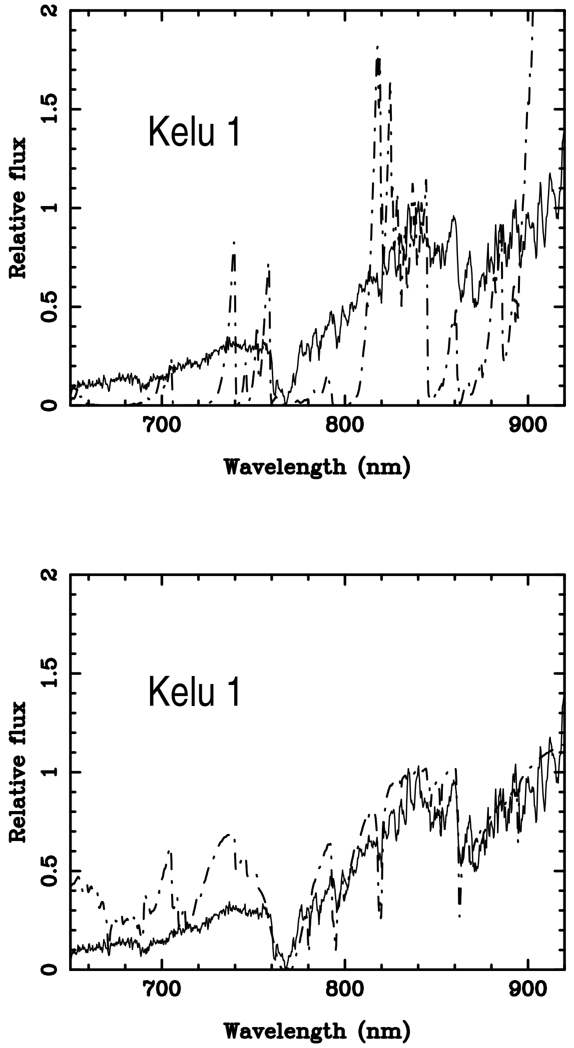

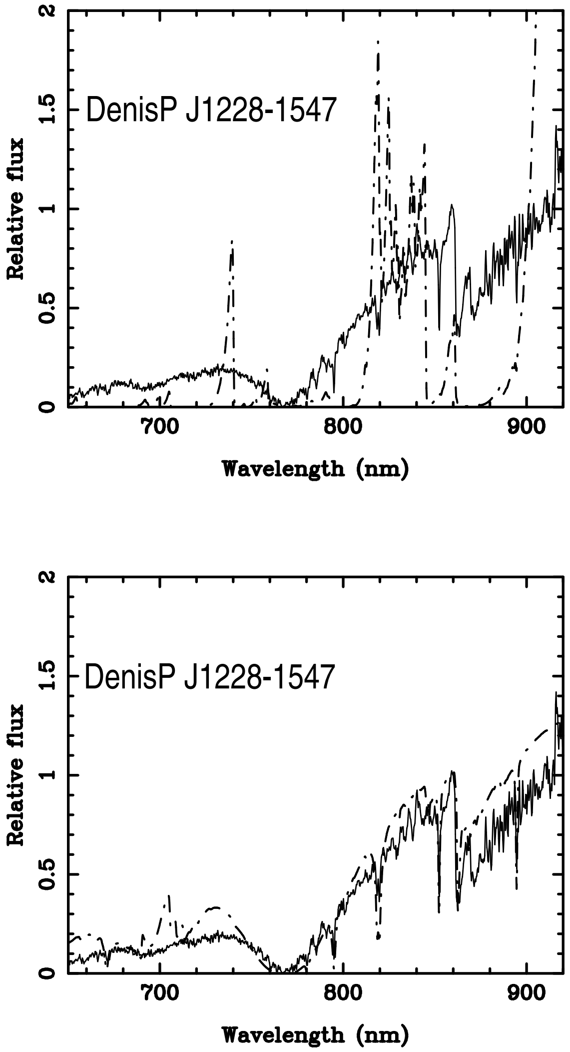

Fig. 4. The observed spectrum of Kelu 1 normalized at ∼840 nm is shown by the full line and the predicted spectra (Tsuji's C-type model atmosphere for $T_{\rm eff} = 2000$ K and $\log g = 5$) are shown by the dash-dotted line at a resolution of 10Å. Upper panel displays the theoretical spectrum computed considering only the natural depletion of molecules as a result of chemical equilibrium. Lower panel depicts the same computations taking into account an "extra" depletion of TiO ($R = 0.01$), VO ($R = 0.08$), CaH ($R = 0.5$) and CrH ($R = 0.2$).

Fig. 5. The observed spectrum of DenisP J1228–1547 normalized at ∼860 nm is shown by the full line and the predicted spectra (Tsuji's C-type model atmosphere for $T_{\rm eff} = 1600$ K and $\log g = 5$) are shown by the dash-dotted line at a resolution of 10Å. Upper panel displays the theoretical spectrum computed considering only the natural depletion of molecules as a result of chemical equilibrium. Lower panel depicts the same computations taking into account an "extra" depletion of TiO ($R = 0.0$), VO ($R = 0.0$), CaH ($R = 0.5$) and CrH ($R = 0.04$).

in the cases of BRI 0021–0214 and Kelu 1. In Fig. 4 (upper panel) we compare the observed spectrum of Kelu 1 with a synthetic spectrum obtained using the Tsuji C-type model for $T_{\rm eff} = 2000$ K and $\log g = 5$. The natural depletion of molecules resulting from the chemical equilibrium is not sufficient to get a reasonable fit to the data. The discrepancies with respect to the observed spectrum can be notably reduced (Fig. 4, lower panel) if we impose a depletion of CaH, CrH, TiO and VO molecules which should account for the condensation of Ca, Cr, Ti and V atoms into dust grains. Since we do not have an appropriate theoretical description of the processes of dust formation at present, we use the simple approach of modifying the chemical equilibrium for all molecules. We implemented this "extra" depletion simply by introducing a factor R which describes the reduction of molecular densities of the relevant species over the whole atmosphere. From the comparison between observed and computed spectra we find that the reduction factor for TiO ranges from 0 (complete depletion) to 1 (i.e. non depletion). In Fig. 5 we can see the comparison of similar synthetic spectra (Tsuji's C-type model atmosphere for $T_{\rm eff} = 1600$ K and $\log g = 5$) with the spectrum of DenisP J1228-1547. Total or almost total depletion of Ti and V into the dust grains is

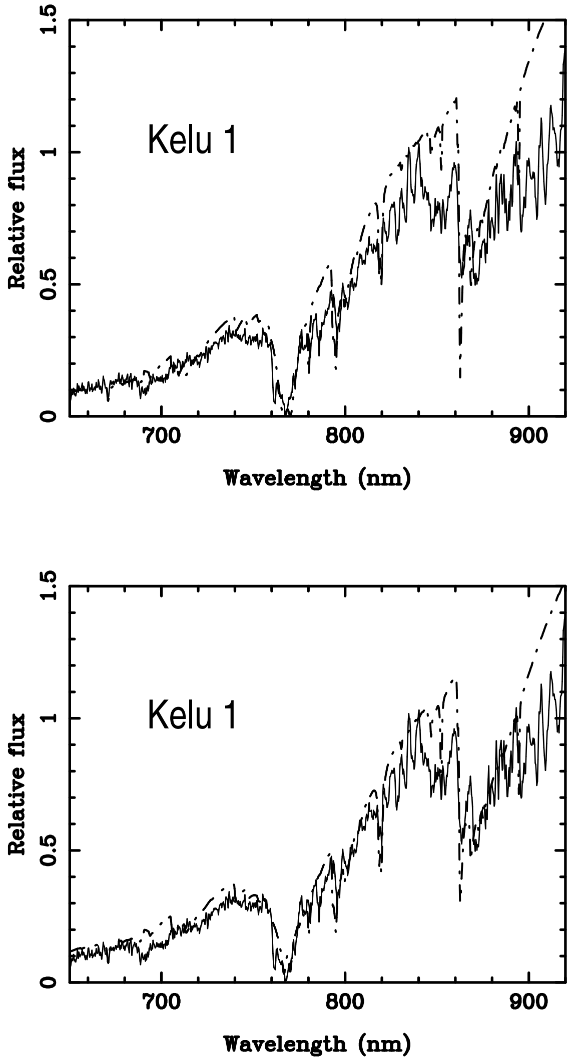

Fig. 6. Kelu 1's observed spectrum (full line) compared to the best fits (dash-dotted line) obtained using Tsuji's (2000) C-type models (upper panel, $T_{\rm eff} = 2000$ K and $\log g = 5$), and Allard's (1999) dusty models (lower panel, $T_{\rm eff} = 1800$ K and $\log g = 5$). Both predicted spectra with a resolution of 10Å have been computed considering the R depletion factors given in Fig. 4 and the AdO law described in the text with $a_\circ = 0.03$.

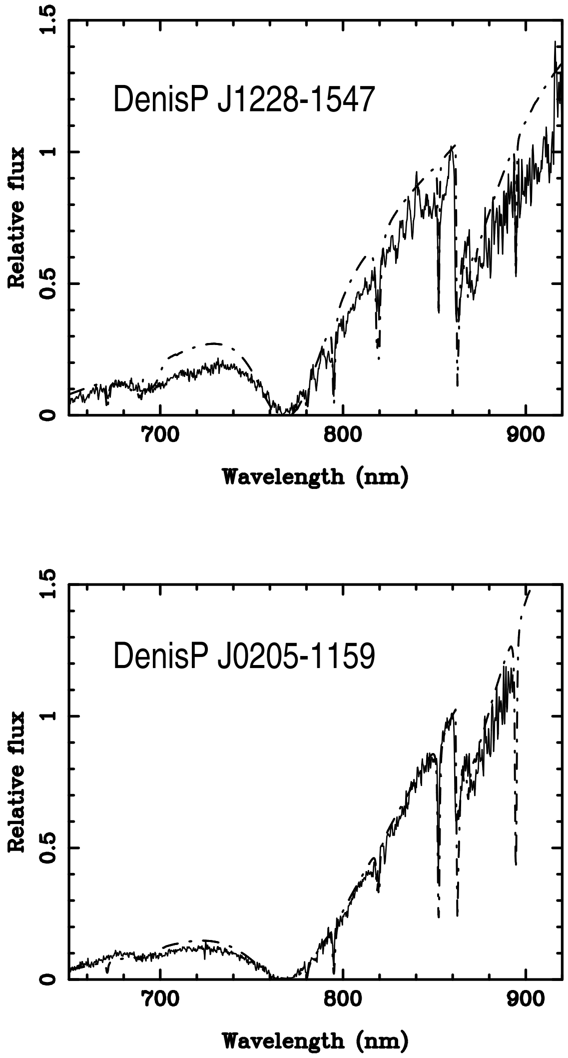

Fig. 7. DenisP J1228–1547 and DenisP J0205–1159's observed data (full line) compared to the best fits (dash-dotted line) obtained using Tsuji's (2000) C-type models (upper panel: $T_{\rm eff} = 1600$ K and $\log g = 5$; lower panel: $T_{\rm eff} = 1200$ K and $\log g = 5$). Both predicted spectra with a resolution of 10Å have been computed considering the R depletion factors given in Fig. 5 and the AdO law described in the text with $a_\circ = 0.006$.

required to explain the spectrum of the mid-type L-dwarfs DenisP J1228–1547 and DenisP J0205–1159.

4.3. The need for additional opacity (AdO)

Our first attempts to model the spectra including atomic and molecular features showed in Figs. 4 and 5 were only modestly successful. Although we could reproduce reasonably well the red wing of the K I line, the theoretical fluxes in the blue part of our synthetic spectra (640–750 nm) are too large. In fact, we cannot fit the observations by taking into account only the opacity provided by the Na I and K I resonance doublets and the continuum opacity sources listed in Table 2.

Since the formation of dust in these cool atmospheres can produce additional opacity (AdO) which may affect the synthetic spectra we decided to investigate whether a simple description of it could help us to improve the comparison between observed and computed spectra. We adopted as law for AdO the following expression: $a_\nu = a_o * (\nu/\nu_0)^N$. For $N = 0$ to 4 this law corresponds to the case of radiation scattering produced by particles of different sizes, being $N = 4$ the case of pure Rayleigh scattering, and $N = 0$ corresponding to the case of white scattering. However, at present we cannot distinguish whether this

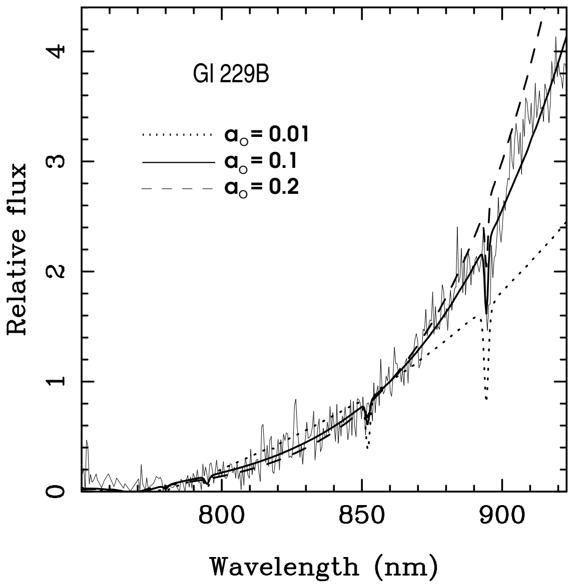

Fig. 8. Gl 229B observed data (thin full line) compared to some predicted spectra obtained using the Tsuji's (2000) C-type model of $T_{\rm eff} = 1000$ K and $\log g = 5$. Different values of $a_\circ$ are oveplotted to show the effect of dust opacity at this low temperature. The best fit is provided by $a_\circ = 0.1$ and $N = 4$. Only Cs I features are seen in the wavelenth range presented here.

AdO is due to absorption or scattering processes. The parameters N and a_0 would be determined from the comparison with observations, but in all cases we try to get the best fit for $N = 4$, which would be the most simple from the physical point of view. We adopted as ν_o the frequency of the K I resonance line at 769.9 nm. Our model of AdO is depth independent and therefore in this approach we cannot model the inhomogeneities (e.g. dust clouds) which may exist in L-dwarf atmospheres.

We have investigated how our simple approach for the modelling of AdO may lead to better comparisons between predicted and observed spectra. The implementation of our law of AdO depresses the fluxes in the blue wing of the K I doublet, considerably improving the reproduction of the observed data of Kelu 1 (Fig. 6), DenisP J1228–1547 (Fig. 7, upper panel) and DenisP J0205–1159 (Fig. 7, lower panel). For each object, synthetic spectra were computed for a range of $T_{\rm eff}$, gravities, a_0 and depletion factors R for TiO, VO, CaH and CrH. The previous figures display those syntheses which better reproduce the observed spectra. From our computations we infer that VO is less efficiently depleted than TiO at a given $T_{\rm eff}$. The depletion of these oxides appears to increase very rapidly as we go from BRI 0021–0214 and Kelu 1 to the lower temperature objects DenisP J0205–1159 and DenisP J0205–1159. Note the good fit to the observed spectra at 860 nm provided by the (0,0) band of the $A^6\Sigma^{(+)}$–$X^6\Sigma^{(+)}$ system of CrH. From the study of this band we also find that the depletion factor of CrH increases from the warmer to the coolest objects in the sample. Finally, we also find that atomic lines become weaker and narrower when increasing the amount of AdO in the atmospheres.

We have also studied whether we can explain the optical spectrum of Gl 229B using the following Tsuji's model: C-type, $T_{\rm eff} = 1000$ K, and $\log g = 5.0$, and the AdO law of index $N = 4$ used above. In Fig. 8 we show several spectral synthesis reproducing the optical spectrum of this object, and showing the effect of different $a_\circ$ parameters which is related to the amount of dust in the atmosphere. In Gl 229B we need the highest value of a_0, which is interpreted as evidence for the most "dusty" atmosphere in our sample. We have not attempted to reproduce the Cs I lines in Gl 229B. According to our hypothesis, the inclusion of AdO avoids the contribution of high pressure regions to the formation of these lines. The shorter wavelength Cs I line at 894.3 nm is very affected by dust opacity.

5. Discussion

5.1. $T_{\rm eff}$ for L-type dwarfs

Our computations provide a reasonable description of the far-red optical spectra of L-dwarfs and provide a physical basis for a progressively decreasing $T_{\rm eff}$ for the proposed spectral classifications (Martín et al. 1999; Kirkpatrick et al. 1999a). Effective temperatures for a few field L-dwarfs and for Gl 229B have been derived from spectra at IR wavelengths (Allard et al. 1996; Marley et al. 1996; Matthews et al. 1996; Tsuji et al. 1999; Jones et al. 1996; Kirkpatrick et al. 1999b). Here we study to what extent we can use the broad energy spectral distribution in the optical to infer the $T_{\rm eff}$ for the cool dwarfs in our sample. Our best estimates using Tsuji's models (see Table 4) are in good agreement with those found from IR data for objects of similar spectral types and for Gl 229B. Using Allard's models and the simple approach of AdO described in section 4.3 we are also able to reproduce the observed spectra, albeit we require lower $T_{\rm eff}$'s by up to several hundred degrees for the coolest L-dwarfs. This is mainly due to the hotter stratification of Allard's model atmospheres for the potassium and sodium lines forming layers (see Fig. 2). Opposite to IR-based temperature determinations, the estimation from optical spectra is very sensitive to the input physics parameters, like dust formation, molecular equilibrium, sources of opacity and atmospheric models, which limits the accuracy of the estimates to $\sim$200 K. On the other hand, the optical spectra provide an opportunity to test the reliability of the physical description of the atmospheres.

Cs I lines in the optical spectra have been recently used to infer the $T_{\rm eff}$ of some L-dwarfs (Basri et al. 1999). In spite of the sensitivity of these lines to many input parameters in the models (i.e. to the amount of opacity, chemical equilibrium, etc.) we find in general a good agreement

Table 4. $T_{\rm eff}$ estimations for our sample adopting Tsuji's (2000) C-type models and $\log g = 5.0$.

Object	Sp. Type	$I - J$	$T_{\rm eff}$ ($\pm$200 K)	Other measures	Source
BRI 0021–0214	M9.5	3.30	2200	1980, 2300	TMR93, LAH98
Kelu 1	L2 (L2)	3.50	2000	2000, 1900	B99, RLA97
DenisP J1228–1547	L4.5 (L5)	3.81	1600	1800	B99
DenisP J0205–1159	L5 (L7)	3.82	1200	1700, 1800	B99, TK99

NOTES. Spectral types are given in Martín et al. (1999). Those spectral types in brackets come from Kirkpatrick et al. (1999a). $(I - J)$ colors have been taken from Leggett, Allard & Hauschildt (1998).
References: TMR93 = Tinney, Mould & Reid (1993); LAH98 = Leggett et al. (1998); B99 = Basri et al. (1999); RLA97 = Ruiz et al. (1997); TK99 = Tokunaga & Kobayashi (1999).

with their estimated temperatures for the earlier L-dwarfs (see Table 4). However, for the latest L-type objects in our sample, DenisP J1228–1547 and DenisP J0205-1159, we find temperatures up to 400 K lower. We may attribute this discrepancy to the effects that dust opacity has in the formation of optical lines of alkalie. This produces a kind of "veiling" of the atomic lines, reducing their intensities. Basri et al. (1999) did not consider this effect, and therefore they required hotter models in order to explain the strength of the observed Cs lines. Another possible reason for the discrepancy is that the temperatures in Table 4 have been obtained for gravity $\log g = 5$; if we increased gravity by 0.5 dex we would have to increase the temperatures of our models by about 200 K. In this case the spectral synthesis does not reproduce the observations so well but they are still acceptable.

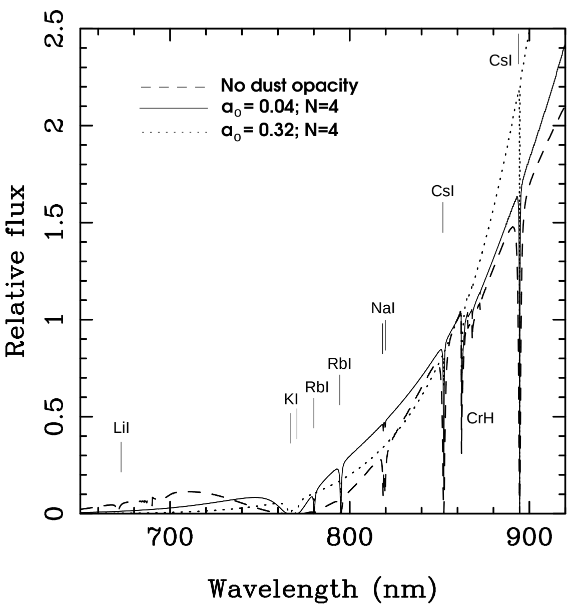

Fig. 9. Predicted optical spectra (Tsuji's C-type model atmosphere, $T_{\rm eff} = 1200$ K and $\log g = 5$) for intermediate objects between Gl 229B and DenisP J0205–1159. Different intensities in the dust opacity have been considered. Spectra have been normalized at 860 nm. Identification of the atomic and molecular bands included in the computations are also provided.

5.2. Alkali lines: the case of lithium

Recently, several new Gl 229B-like objects have been discovered by the SDSS survey (Strauss et al. 1999) and the 2MASS collaboration (Burgasser et al. 1999). Based on their near-IR spectra, these authors suggest that these new cool brown dwarfs may be warmer than Gl 229B. In order to estimate the optical properties of these objects we have computed synthetical spectra using a Tsuji's C-type model of $T_{\rm eff} = 1200$ K and $\log g = 5.0$, and we have adopted the basic prescriptions that were followed in section 4, i.e total depletion of VO and TiO and the AdO law with $N = 4$. In Fig. 9 we plot the resulting spectra considering different amounts of dust opacity. As expected, the overall shape of the spectrum is intermediate between that of DenisP J0205–1159 and Gl 229B. In the absence of dust absorption ($a_\circ = 0.0$) alkali lines are clearly seen (including the lithium resonance doublet), and the spectrum is governed by the sodium and potassium lines. If we consider dust opacities comparable to those in Gl 229B, the alkali lines of Cs and Rb become weaker, but still detectable with intermediate resolution spectroscopy. Remarkably, the subordinate Na I doublet at 819.5 nm is very sensitive to the incorporation of dust opacity due to the larger depths of its formation as compared with resonance lines. For very high dust opacities these lines may become undetectable.

The effects of additional dust opacity on the formation of Li I lines (resonance and subordinate ones) also deserve detailed consideration since they play a major role as a discriminator of substellar nature for brown dwarf candidates (see Rebolo, Martín, & Magazzù 1992; Magazzù, Martín, & Rebolo 1993). Most of the known brown dwarfs are actually recognized by the detection of the Li I resonance doublet in their spectra (Rebolo et al. 1996; Martín et al. 1997a; Rebolo et al. 1998; Tinney 1998; Kirkpatrick et al. 1999a). The chemical equilibrium of lithium contained molecules have been considered in all our syntheses (Fig. 10 depicts the density profiles for lithium species for two C-type models by Tsuji 2000). Our computations

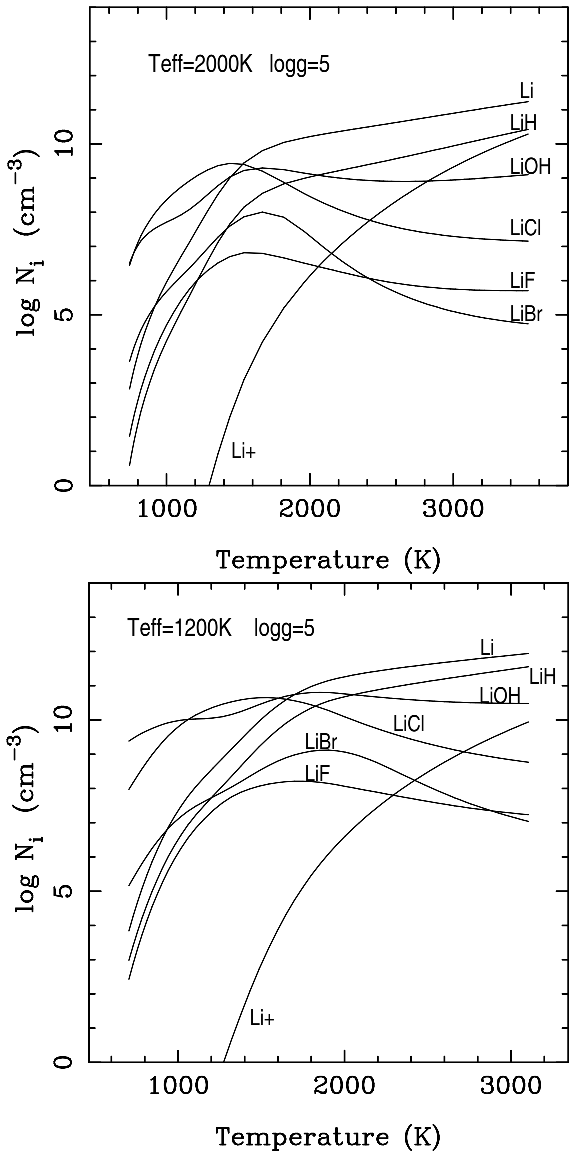

Fig. 10. Densities of lithium and the most abundant species containing lithium are plotted for the C-type Tsuji's (2000) model atmospheres with $T_{\rm eff} = 2000$ K (upper panel) and 1200 K (lower panel) and $\log g = 5$. Computations have been performed under the assumption of complete chemical equilibrium for a solar elemental mixture.

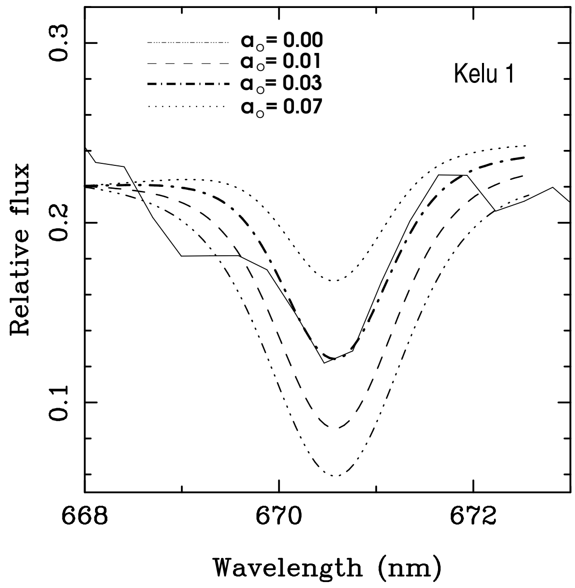

Fig. 11. Fitting of the Li I resonace line of Kelu 1 (full line) using the Tsuji's C-type model atmosphere for $T_{\rm eff} = 2000$ K, $\log g = 5$. Computations have been performed for a lithium abundace of $\log N(\rm Li) = 3.0$ and considering different amounts of dust opacity. The resolution of all theoretical spectra is the same than the one of the observed data. The predicted model that better fits the observations coincides with the one that also nicely reproduces the overall shape of the optical spectrum ($a_\circ = 0.03$, see Fig. 6).

show that both, the resonance line at 670.8 nm, and the subordinate lines at 601.3 nm and 812.6 nm are very sensitive to the AdO that we need to incorporate in the spectral synthesis if we want to explain the observed broad spectral energy distribution. Among the subordinate lines the doublet at 812.6 nm is more easily detectable, but the predicted EWs, assuming fully preserved lithium, are rather small, ranging from EW = 0.4Å to 0.04Å for $T_{\rm eff}$ values in the range 2000 K down to 1200 K. These EWs are considerably reduced by the inclusion of the AdO described in the previous section, which makes their detection rather difficult. In Table 5 we give the predicted EWs of the Li I resonance doublet at 670.8 nm for several of the coolest model atmospheres (2000–1000 K) considered in this work. First, we note that in the absence of any AdO (second column in the table), we would expect rather strong neutral Li resonance lines in the spectra of objects as cool as DenisP J0205–1159 and Gl 229B. The chemical equilibrum of Li-contained species still allow a sufficient number of Li atoms to produce a rather strong resonance feature; one reason for this is that Cl and O atoms should be also bounded into other molecules (e.g. NaCl, KCl, H_2O, etc.). Our computations indicate that objects like DenisP J0205–1159 and cooler objects with moderate dust opacities should show the Li I resonance doublet if they had preserved this element from nuclear burning, and consequently the lithium test can still be applied. Furthermore, even in very dusty cool atmospheres like that of Gl 229B for which we have inferred a high value of the opacity parameter of $a_\circ = 0.1$ (fourth column in Table 5), the lithium resonance line could be detected with an EW of several hundred mÅ (high S/N data would be required).

Another effect that we shall consider is whether small changes in the AdO (which could be originated as a consequence of some "meteorological" phenomena occurring in these cool atmospheres) can lead to detectable variations

Table 5. Equivalent widths (Å) of the Li I resonance doublet at 670.8 nm computed for the C-type Tsuji's (2000) model atmospheres, cosmic Li abundance ($\log N(\mathrm{Li}) = 3.2$) and gravity $\log g = 5.0$.

T_{eff}	$a_\circ$		
	0.00	0.01	0.10
(K)	EW (Å)		
1000	17	8	0.6
1200	30	12	0.7
1400	42	21	0.9
1600	40	24	1.6
2000	23	16	3.6

in the EWs of the lithium lines. In particular, weak lithium lines do not necessarily imply a depletion of this element. The observed Li I variability in Kelu 1 (with changes in EW by a factor 5), could be an indication of meteorological changes in the atmosphere of this rapidly rotating cool object. In Fig. 11 we present several spectral synthesis showing the sensitivity of the lithium line to the AdO in the atmosphere. The AdO parameters which give the best fit for the lithium line in Kelu 1 (EW = 6.5±1.0 Å) coincide with those also providing the best fit to the whole optical spectrum (see Fig. 6). Anyway, the obtained lithium abundance is consistent with complete preservation of this element.

6. Conclusions

In this paper we have attempted to model the far-red spectra (640–930 nm) of several L-dwarfs suitably selected to cover this new spectral class. We have used model atmospheres from Tsuji (2000) and Allard (1999), as well as an LTE spectral synthesis code (Pavlenko et al. 1995) which takes into account chemical equilibrium for more than 100 molecular species, and detailed opacities for the most relevant bands. We have arrived to the following conclusions:

1) Alkali lines play a major role governing the far-red spectra of L-dwarfs. At early types, this role is shared with TiO and VO bands, which dominate this spectral region in late M-dwarfs. As we move to later spectral types we need to incorporate progressively higher depletions of these oxides and of the hydrides CrH and CaH, consistently with the expectation that Ti and V atoms are depleted into grains; and we also require additional opacity to reproduce the overall shape of the spectra. This additional opacity could be either due to molecular/dust absorption or to dust scattering.

2) We have shown that a simple law for this additional opacity of the form $a_\circ\ (\nu/\nu_\circ)^N$, with $N = 4$, gives a sufficiently good fit to the observed spectra of L-dwarfs and Gl 229B. For this late object we require the highest value of $a_\circ$ consistent with a very dusty atmosphere. The strength of alkali lines is highly affected by this opacity.

3) From the best fits to our spectra, we derive the most likely T_{eff} values for our sample of L-dwarfs. For the warmer objects, our values are consistent with those obtained by other authors, however we find lower T_{eff}'s by serveral hundred degrees for the coolest L-dwarfs. Because the optical spectra are very much affected by the input physics, a more reliable T_{eff} scale should be obtained by fitting the IR data of these cool objects.

4) After detailed consideration of chemical equilibrium, we find that the lithium resonance doublet at 670.8 nm can be detected in the whole spectral range (down to 1000 K). In the coolest L-dwarfs the strength of the resonance line is more affected by the amount of additional opacity needed to explain the spectra than by the depletion of neutral lithium atoms into molecular species. In those atmospheres where the additional opacity required is low, the lithium test can provide a useful discrimination of substellar nature. Changes in the physical conditions governing dust formation in L-dwarfs, will cause variability of the lithium resonance doublet. Taking into account the need for additional opacity in Kelu 1, we find that the lithium abundance can be as high as $\log N(\mathrm{Li}) = 3.0$, i.e. consistent with complete preservation.

Acknowledgements. We thank T. Tsuji, F. Allard, D. Schwenke, G. Schultz and B. Oppenheimer for providing us model atmospheres, updated TiO molecular data and the optical spectrum of GL 229B, respectively. We are also indebted to R. García López, Gibor Basri and Eduardo L. Martín for their assistance with the observations. Partial financial support was provided by the Spanish DGES project no. PB95-1132-C02-01.

References

Allard, F. 1999, private communication
Allard, F., Hauschildt, P. H. 1995, ApJ, 445, 433
Allard, F., Hauschildt, P. H., Baraffe, I., Chabrier, G. 1996, ApJ, 465, L123
Allard, F., Hauschildt, P. H., Alexander, D. R., Starrfield, S. 1997, ARA&A, 35, 137
Basri, G., et al. 1999, ApJ, in press
Burgasser, et al. 1999, ApJ, 522, L65
Cymbal, V. V. 1977, in Tables of the Franc-Condon factors with account of vibraton-rotational interaction for astrophysically important molecules. I. Titanium oxide, deposited N 246–77
Delfosse, X., Tinney, C. G., Forveille, T., et al. 1997, A&A, 327, L25
Gurvitz, L. V., Weitz, I. V., Medvedev, V. A. 1982, Thermodynamic properties of individual substances. Moscow. Science
Huber, K. P., Herzberg G. 1979, in Constants of Diatomic Molecules, Van Nostrand Reinhold, N. Y.
Irwin, M., McMahon, R. G., Reid, N. 1991, MNRAS, 252, 61
Israelian, G., García López, R., Rebolo, R. 1998, ApJ, 507, 805
Jones, H. R. A., Longmore, A. J., Allard, F., Hauschildt, P. H. 1996, MNRAS, 280, 77
Jones, H. R. A., & Tsuji, T. 1997, ApJ, 480, L39

Kirkpatrick, J. D., Allard, F., Bida, T., Zuckerman, B., Becklin, E. E., Chabrier, G., Baraffe, I. 1999b, ApJ, 519, 834
Kirkpatrick, J. D., Reid, I. N., Liebert, J., et al. 1999a, ApJ, 519, 802
Kurucz, R. L. 1993, CD ROM #9, Cambridge, MA: Smithsonian Astrophysical Observatory
Leggett, S. K., Allard, F., Hauschildt, P. H. 1998, ApJ, 509, 836
Lunine, J. I., Hubbard, W. B., Burrows, A., Wang, Y.-P., Garlow, K. 1989, ApJ, 338, 314
Magazzù, A., Martín, E. L., Rebolo, R. 1993, ApJ, 404, L17
Marley, M. S., Saumon, D., Guillot, T., Freedman, R. S., Hubbard, W. B., Burrows, A., Lunine, J. I. 1996, Science, 272, 1919
Martín, E. L., Basri, G., Delfosse, X., Forveille, T. 1997a, A&A, 327, L29
Martín, E. L., Delfosse, X., Basri, G., Goldman, B., Forveille, T., Zapatero Osorio, M. R. 1999, AJ, in press (November issue)
Martín, E. L., Pavlenko, Ya. V., ,Rebolo, R. 1997b, A&A, 326, 731
Martín, E. L., Rebolo, R., Zapatero Osorio, M. R. 1996, ApJ, 469, 706
Matthews, K., Nakajima, T., Kulkarni, S. R., Oppenheimer, B. R. 1996, AJ, 112, 1678
Nakajima, T., Oppenheimer, B. R., Kulkarni, S. R., Golimowski, D. A., Matthews, K., Durrance, S. T. 1995, Nature, 378, 463
Oke, J. B., et al. 1995, PASP, 107, 375
Oppenheimer, B. R., Kulkarni, S. R., Matthews, K., Nakajima, T. 1995, Science, 270, 1478
Osterbrock, D. E., Fulbright, J. P., Martel, A. R., Keane, M. J., Trager, S. C., Basri, G. 1996, PASP, 108, 277
Pavlenko, Ya. V, 1997, Astron. Reports, 41, 537
Pavlenko, Ya. V. 1998, Astron. Reports, 42, 787
Pavlenko, Ya. V. 1999a, Astron. Reports, 43, 115
Pavlenko, Ya. V. 1999b, Astron. Reports, in press
Pavlenko, Ya. V., Rebolo, R., Martín, E. L, García López, G. A&A, 303, 807.
Pavlenko, Ya. V., Zapatero Osorio, M. R., Rebolo, R. 2000, in Low-Mass Stars and Brown Dwarfs in Stellar Clusters and Associations, La Palma, CUP, in press
Piskunov, N. E., Kupka, F., Ryabchikova, T. A., Weiss, V. V., Jeffery, C.S. 1995, A&AS , 112, 525
Rebolo, R., Martín, E. L., Magazzù, A. 1992, ApJ, 389, L83
Rebolo, R., Martín, E. L., Basri, G., Marcy, G. W., Zapatero Osorio, M. R. 1996, ApJ, 469, L53
Rebolo, R., Zapatero Osorio, M. R., Madruga, S., Béjar, V. J. S., Arribas, S., Licandro, J. 1998, Science, 282, 1309
Ruiz, M. T., Leggett, S. K., Allard, F. 1997, ApJ, 491, L107
Schwenke, D. 1998, in Chemistry and Physics of Molecules and Grains in Space. Faraday Discussions No. 109. The Faraday Division of the Royal Society of Chemistry, London, p. 321
Schultz, A. B., Allard, F., Clampin, M., et al. 1998, ApJ, 492, L181
Schumaker, J.B. 1969. JQSRT, v. 9, p. 153
Strauss, M. A., et al. 1999, ApJL, 522, L61
Tinney, C. G. 1998, MNRAS, 296, L42
Tinney, C. G., Mould, J. R., Reid, I. N. 1993, AJ, 105, 1045
Tokunaga, A. T., Kobayashi, N. 1999, AJ, 117, 1010
Tsuji, T. 1973, A&A, 23, 411
Tsuji, T. 2000, in Low-Mass Stars and Brown Dwarfs in Stellar Clusters and Associations, La Palma, CUP, in press
Tsuji, T., Ohnaka, K., Aoki, W. 1996a, A&A, 305, 1
Tsuji, T., Ohnaka, K., Aoki, W. 1999, ApJ, 520, L119
Tsuji, T., Ohnaka, K., Aoki, W., Nakajima, T. 1996b, A&A, 308, 29
Yakovina, L. A., Pavlenko, Ya. V. 1998, Kinemat. and Phys. of Celest. Bodies, 14, 195